Deposition and characterisation of bismuth oxide thin films

V. Fruth [a,*], M. Popa [b], D. Berger [c], R. Ramer [d], M. Gartner [a], A. Ciulei [a], M. Zaharescu [a]

[a] *Institute of Physical Chemistry, Spl.Independentei 202, Bucharest 66021, Romania*
[b] *Tokyo Institute of Technology, Nagasuta 4259, Midori-ku, Yokohama 226-8503, Japan*
[c] *"Politehnica" University Bucharest, 1 Polizu Street, 78126 Bucharest, Romania*
[d] *University of New South Wales, Sydney 2052, NSW Australia*

Available online 23 March 2005

Abstract

Owing to their peculiar characteristics, bismuth oxides are used in various domains, such as microelectronics, sensor technology, optical coatings, transparent ceramic glass manufacturing, etc. Bismuth oxide system exhibit high oxide ionic conductivity and have been proposed as good electrolyte materials for application, such as solid oxide fuel cell (SOFC) and oxygen sensor.

Antimony doped and undoped Bi_2O_3 films were deposited onto glass substrate from bismuth nitrate and antimony precursor solutions. As chelating agent polyethyleneglycol (PEG) was used and the above-mentioned precursor solutions were sufficiently viscous.

In the present paper, the formation of different phases belonging to the Bi–O system during thermal treatments of the Bi-based films is investigated by means of spectroscopic ellipsometry (SE), polarising microscope observation, X-ray diffractometry (XRD), and infrared spectrometry (IR). The thickness and the porosity of the films were evaluated. These preparation techniques, differing mainly in precursor materials and method of deposition, lead to different quality of the resulting films.
© 2005 Elsevier Ltd. All rights reserved.

Keywords: Sol–gel processes; X-ray methods; Optical properties; Bi_2O_3; Functional application

1. Introduction

Ceramic films are essential for devices because the intrinsic properties of the material, rather than its grain boundaries, can be exploited. Cubic bismuth oxide has the highest known oxide ion mobility, which makes it useful for fuel cells, sensors of various types, electrolyzers and ceramic membranes for high-purity oxygen separation and partial oxidation of hydrocarbons.[1–5] Nonequilibrium crystal structures can be stabilized by producing nanometer-scale crystallites or by epitaxially depositing the material onto a template with a crystal structure similar to the one desired. Switzer et al.[1] used electrodeposition to produce nonequilibrium-layered nanostructures and superlattices of metal oxides that showed quantum confinement effects. They have shown that single-crystal films of the high-temperature cubic polymorph of bismuth oxide δ-Bi_2O_3 can be epitaxially electrodeposited.

Unfortunately, the cubic structure is only stable from 705 to 740 °C to the melting point at 825 °C. The variation of the transition temperature in such a wide range is related to the purity of samples, their thermal pre-history and oxygen stoichiometry.[2–5] At ambient temperature a monoclinic form, α-Bi_2O_3 phase, is stable. Each polymorph possesses distinct crystalline structures and physical properties[2,4–10] (electrical, optical, photoelectrical, etc.). For example, at 300 K, the band gap of monoclinic α-Bi_2O_3 is equal to 2.85 eV, while that of tetragonal β-phase is 2.58 eV.[11]

The conductivity drops by over three orders of magnitude at temperatures less than 729 °C, when the material transforms to the monoclinic α-Bi_2O_3 form.[2,4,5,9] Furthermore, the volume change that is associated with the δ-phase → α-phase transition produces cracking associated with phase transformation during cyclic heating and cooling and severe deterioration of the material, and the oxide tends to reduce to Bi metal at the high temperatures and reducing conditions of conventional fuel cells.[1,2,8] The cubic structure can be stabilized by the addition of rare-earth metal ions,[2,5,8] but the conductivity drops by about two orders of magnitude. The cu-

* Corresponding author.
 E-mail address: vfruth@icf.ro (V. Fruth).

bic crystal structure of δ-Bi_2O_3 is a defect fluorite structure with disordered occupancy of the cation sites and disordered vacancies on the oxygen sites.[7,10] A metastable phase, β-Bi_2O_3, exhibits oxygen ion conductivity that is much higher than yttria-stabilized ZrO_2 (YSZ) up to the maximum operating temperature of about 800 °C.

The present study is devoted to synthesis and characterisation of bismuth oxide films. A wet chemical route is adopted to obtain doped and undoped thin Bi_2O_3 films. Sb^{3+} ion was used as dopant due to its similar sterical behaviour and smaller ionic radius.

2. Experimental

Thin bismuth oxide films, antimony doped ($Bi_{1.9}Sb_{0.1}O_3$) and undoped were deposited onto a glass substrate following the sol–gel aqueous route. As precursors $Bi(NO_3)_3 \cdot 5H_2O$ (98% in purity) and Sb_2O_3 (99% in purity) were used. The 0.1 M $Bi(NO_3)_3$ solution (labelled B) was prepared by dissolving 4.9 g $Bi(NO_3)_3 \cdot 5H_2O$ into 100 ml (1:5 HNO_3:H_2O). Polyethyleneglycol (PEG) 200 solution was added as chelating agent. The 0.1 M antimony solution (labelled S) was prepared by dissolving Sb_2O_3 in citric acid (CA) solution. The as above prepared solutions were mixed (95%:5% volume fraction B:S) subsequently degassed using N_2, and finally a transparent solution (labelled BS) resulted. From these solutions (B and BS), the films were deposited on silica-soda-lime glasses by dipping using a withdrawal rate of 5 cm/min. Both solutions used for film deposition were left for gelatin, either at room temperature or in a dry oven at 100 °C and subjected to differential thermal analysis and thermogravimetric analysis (DTA/TGA), using a MOM–OD 103 Derivatograph, in order to establish the thermal treatment schedule.

The films were preliminary thermally treated with a heating rate of 1 °C/min at 450 and 600 °C, respectively where a 1 h plateau was maintained.

Characterisation of the films was performed using X-ray diffraction (XRD), spectroscopic ellipsometry (SE) and polarising microscope observation. The structural and optical characterisation of the films (SE) were carried out in air, in the 300–700 nm wavelength range at an angle of incidence of 75°. The acquisition interval of the data was 10 nm and the reading accuracy of azimuths was 1 min. The dielectric function of the Bi_2O_x layer can be calculated using the Bruggeman-effective medium approximation[12] (B-EMA) if the layer can be considered as microscopically heterogeneous but macroscopically homogeneous materials, which consists of a mixture of separated phases. The optical model used in this work consists of one layer on the substrate (glass).

3. Results and discussions

The crystalline structure of bismuth oxide films strongly depends on the nucleation and growth processes at

film–substrate interface and is mainly determined by the crystalline structure of the substrate. If this is amorphous, then a bismuth oxide layer of the same nature is expected to form up at the structure interface. A homogenous germination of different crystalline phases of Bi–O system takes place on the newly formed amorphous layer and among them the phase with lowest free energy will be predominant.[13]

The DTA/TG analysis results of the dried gels obtained from the S and BS solution show a thermal decomposition in steps.[14] The adsorbed water, nitric radicals as well as the organic residues were eliminated below 500 °C. Two exothermal at 190 and 290 °C were noticed. Therefore, a thermal schedule ranging between 500 and 800 °C is convenient to crystallise the Bi_2O_3. Preliminary annealing treatments at 450 and 600 °C were established. The infrared spectrometry (IR) spectra were recorded in order to obtain more data about structure of the prepared precursors.[14] In this stage of preparation one can note the presence of characteristic vibration modes of NO_3^-, OH^-, COO^-. The presence in small quantities of dopant (Sb^{3+}) produced significant changes especially in the range 1000–2000 cm^{-1}. This fact underlined structural changes of the gels in the early stage of preparation induced by the presence of dopant.

The films after deposition were amorphous as determined by XRD and microscopic observation. All the coatings thermally treated at 450 °C for 1 h were X-ray amorphous. Only polarising microscope observation underlined some inhomogeneous structural changes. Figs. 1 and 2 show the XRD patterns of multilayered coatings. It is observed that the single layer shows almost no peak of a crystallised phase for both investigated compositions. A higher number of depositions means a higher number of thermal treatments, which lead to a densification, followed by porosity decrease. At the same time, multiplied thermal treatments lead to changes in the crystallite size and due to their rearrangement in the network it is possible to determine the void formation, which increase the porosity of film. One can notice the influence of dopant
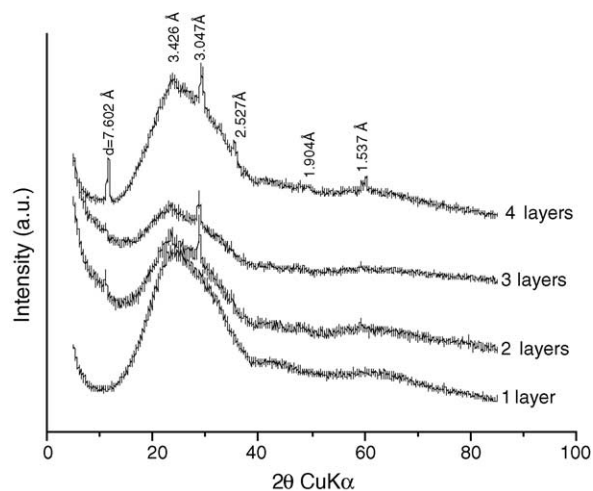

Fig. 1. XRD pattern of the undoped films (B solution) onto glass substrate after consequent annealing treatment 1 h/600 °C.
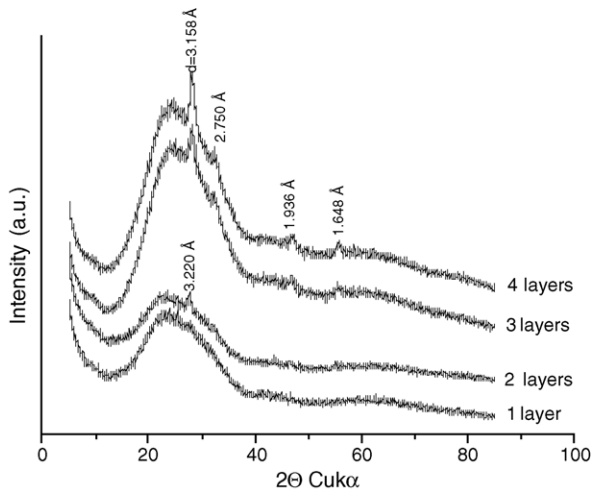
Fig. 2. XRD pattern of the antimony doped films (BS solution) onto glass substrate after consequent annealing treatment 1 h/600 °C.

on the crystallisation process: (i) in the case of undoped films, presented patterns, which can be indexed as a tetragonal phase with c parameter 10 order higher ($a = 3.79$ Å and $c = 30.87$ Å for four layers), infer the presence of a higher oxygen deficient phase[6] (close to $Bi_2O_{2.33}$); (ii) the antimony doped film patterns underlined a general change of the symmetry (from tetragonal to cubic) as the number of annealing treatments and layers increased. The diffraction patterns can be assigned to a mixture of two phases, one tetragonal with deficit in oxygen-β-phase and one cubic, in formation, δ-phase.

Characterisation of the films was performed using spectroellipsometric (SE) measurements. The parameters of the fit were the thickness of the layers and the volume fraction of the components. From the best fit one obtained the refractive index (n) (Fig. 3), the thickness of the layers (d) and volume fractions of the components (Table 1). The error reported in the table was calculated according to Eq. (1)

$$\text{Error} = \sum_{i=1}^{N} \frac{[(R_i^{ec} - R_i^{em})^2 + (I_i^{mc} - I_i^{me})^2]}{N} \qquad (1)$$
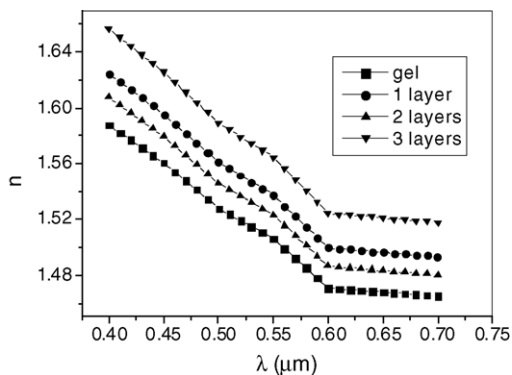

Fig. 3. The refractive index for undoped samples with 1, 2 and 3 layers in the visible wavelength range from ellipsometric analysis.
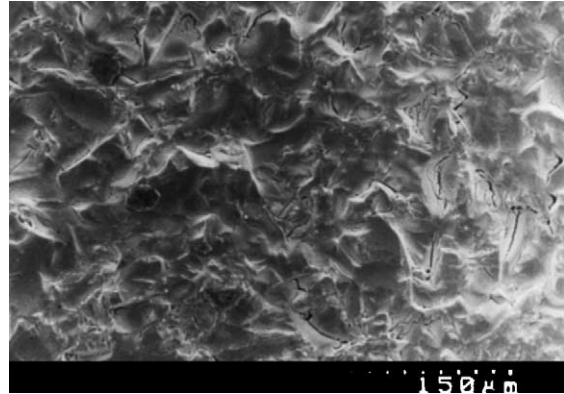

Fig. 4. SEM image of the doped ceramic film with three layers after consecutive annealing treatment.

where R_e is the real part of ellipsometric function ($\tan \Psi \cos \Delta$); R_i^{ec}, the calculated value; R_i^{em}, the measured value; I_m, the imaginary part of ellipsometric function ($\tan \Psi \sin \Delta$); I_i^{mc}, the calculated value; I_i^{me}, the measured value; N, the number of experimental points.

The Wemple-Di Domenico (WDD) model[15] was used to fit the refractive index dispersion in the region of transparency (at low energy) to obtain the direct optical gap of the sol–gel film. In their model, the refractive index is described by the relation (2):

$$n^2(\omega) - 1 = \frac{E_d E_o}{E_o^2 - E^2} \qquad (2)$$

where E_d is the dispersion energy, a measure of the average strength of the interband optical transitions (associated with the changes in the structural order of the material); E_o, the oscillation energy, which is related to the optical gap by the empirical formula[16] $E_o = 1.5E_g$.

After the thermal treatment at 600 °C, the film is densified, the thickness decreases and refractive index increases. Interpretation of the experimental data is in progress.

In all the cases, the thickness of the films increases with the number of the layers (Table 1). It can be observed that the higher number of the layers implied successive thermal treatments, which produce a progressive decrease in the porosity. The optical gap decreases also with the densification of the film.

The image shown below (Fig. 4) represents a microscopic observation (SEM) of the film obtained from BS solution and deposited on glass substrate with four layers. Some microcracks can be noticed and also an irregular surface caused by the processing steps. This film may consist of misoriented microdomains, with defects, such as stacking faults at the domain boundaries. The microscopic observations are in good agreement with the ellipsometric data and confirmed the thickness of the films in this stage of processing. More prolonged annealing treatment at higher temperatures are necessary.

Table 1
Thickness (*d*), volume fractions of the components and band gap energy (*E*$_g$) of B (Bi$_2$O$_3$ + PEG) films

Sample	No. of layers	No. of treatments	d (Å)	Bi$_2$O$_3$ (%)	Air (%)	E_g (eV)	E_d (eV)	Error
B (gel)	1	–	1620	49.95	50.05	2.57	3.22	0.000566
B	1	1	1449	52.66	47.34	2.49	3.24	0.000807
B	2	2	2674	51.42	48.58	2.49	3.15	0.002593

4. Conclusions

The present study is devoted to the synthesis and characterisation of bismuth oxide films. A wet chemical route was adopted to obtain doped and undoped thin Bi$_2$O$_3$ films. The presence of dopant (Sb^{3+}) produced significant changes of the gels in the early stage of preparation and promotes different route of crystallisation of the thin films. According to the ellipsometric results, the as above deposited films on the glass substrate had a thickness of hundreds Å. Detailed investigation on the compositions and microstructure of the films are in progress.

This synthetic strategy represent a viable alternative to obtain thin films of good qualities and a starting point for tailoring new ceramic materials.

References

1. Switzer, J. A., Shumsky, M. G. and Bohannan, E. W., Electrodeposited ceramic single crystals. *Sience*, 1999, **284**, 293–296.
2. Kharton, V. V., Naumovich, E. N., Yaremchenko, A. A. and Marques, F. M. B., Research on the electrochemistry of oxigen ion conductors in the former Soviet Union. IV. Bismuth oxide-based ceramics. *J. Solid State Electrochem.*, 2001, **5**, 160–187.
3. Sammes, N. M., Tompsett, G. A., Nafe, H. and Aldinger, F., Bismuth based oxide electrolytes-structure and ionic conductyvity. *J.Eur. Ceram. Soc.*, 1999, **19**, 1801–1826.
4. Boivin, J. C., Structural and electrochemical features of fast ion conductors. *Int. J. Inorg. Mater.*, 2001, **3**, 1261.
5. Goodenough, J. B., Oxide-ion electrolytes. *Ann. Rev. Mater. Res.*, 2003, **33**, 91–128.
6. Medernach, J. W. and Snyder, R. L., Powder diffraction patterns and structures of the bismuth oxides. *J. Am. Ceram. Soc.*, 1978, **61**, 494–497.
7. Wachsman, E. D., Boyapati, S., Kaufman, M. J. and Jiang, N., Modeling of ordered structures in phase-stabilized cubic bismuth oxide. *J. Am. Ceram. Soc.*, 2000, **83**, 1964–1968.
8. Shuk, P., Wiemhöfer, H. D., Guth, U., Göpel, W. and Breenblatt, M., Oxide ion conducting solid electrolytes based on Bi$_2$O$_3$. *Solid State Ionics*, 1996, **89**, 179–196.
9. Boivin, J. and Mairesse, C., Recent material development in fast oxide ion conductors. *Ichem. Mater.*, 1998, **10**, 2870–2888.
10. Yashima, M. and Ishimura, D., Crystal structure and disorder of tast oxide-ion conductor cubic Bi$_2$O$_3$. *Chem. Phys. Lett.*, 2002, **378**, 395–399.
11. Leontie, L., Caraman, M., Alexe, M. and Harnagea, C., Structural and optical characteristics of bismuth oxide thin.films. *Surf. Sci.*, 2002, **507**, 480–485.
12. Bruggeman, D. A. G., Berechnung verschiedener physikalischer Konstanten von heterogenen Substanzen. *Ann. Phys.*, 1935, **24**, 636–679.
13. Thompson, C. V., Structure evolution during processing of polycrystaline films. *Ann. Rev. Mater. Sci.*, 2000, **30**, 159–189.
14. Fruth, V., Popa, M., Berger, D., Predoana, L., Gathner, M. and Zaharescu, M., Antimony doped Bi$_2$O$_3$ thin films. *Key Eng.*, 2004, **264–268**, 1245–1248.
15. Wemple, S. H. and DiDomenico Jr., M., Behavior of the electronic dielectric constant in covalent and ionic materials. *Phys. Rev. B*, 1971, **3**, 1338–1351.
16. Solomon, I., Schmidt, M. P., Senemaud, C. and Khodja, M. D., Band structure of carbonated amorphous silicon studied by optical, photoelectron, and X-ray spectroscopy. *Phys. Rev.*, 1988, **B38**, 13263–13270.